INTERNATIONAL CONFERENCE ON
Contemporary Science Technology & Management
7th & 8th April 2020 - ICCSTM

MOBliF: Multi Scale Optimal Blind Transmission Map Fusion and Restoration CNN for Effective Video Dehazing

B.Bhaskar Reddy, Research Scholar , Dr.B.Ramamurthy,professor,S.K.Univesity,Ananthapuram

***Abstract*— Video dehazing has a huge demand in intelligent transportation, advanced driver assistance systems (ADAS), long-range surveillance, object tracking, lane departure detection, autonomous aerial vehicles and endoscopic surgery. But the traditional techniques which are available for dehazing are lagged with over saturates the dehazed image, constant atmospheric light model, not compact to uneven haze. In this paper, we proposed the efficient and adaptive identification and removal of haze from the video by integrating the Multi scale fusion concept into the transmission maps refinement. And also we have the model of atmospheric light estimation using internal patch recurrence which is strong prior for blind dehazing of the video frames to solve a various ill-posed visual issues. Transmission map estimation unit in our system has two models. One is that optimal transmission map computation under a heuristic assumption in the dehazing model to preserve the depth consistency of the frame. Second is that dark Channel Prior based transmission map prediction for multiple scales. With the constraints on the solution space, we then incorporate two scene priors, including locally consistent scene radiance and context-aware scene transmission, to formulate a constrained minimization problem and solve it by quadratic programming. We propose a Multi-scale Optimal Fusion (MOF) model to fuse pixel-wise and patch-wise transmission maps optimally to avoid misestimated transmission region. This MOF is then embedded into patch-wise dehazing to suppress halo artifacts. Quantitative and Qualitative results of proposed algorithm are computed and compared with the existing methods. These performance analysis shows that our proposed algorithm achieves the noteworthy improvements over the previous methods.**

***Index Terms*—Video dehazing, Dark Channel Prior, Atmoshpheric Light, Transmission Map, Multi Scale Fusion.**

I. INTRODUCTION

Nowadays photos have become an inevitable part of our lives. The purpose may vary with the situations. The light received on an image acquisition device gets deteriorated due to the presence of haze, mist, fog, dust, and smoke. These tiny particles absorb and scatter radiance traveling from an object point to the observer plane. This phenomenon not only reduces object visibility but also hampers color fidelity and ontrast of the scene [1]. Haze, fog and even underwater scattering are such phenomena, whose degradation effect on the resulting images grows with scene depth [2]. This degradation is due to dual factors: (i) the irradiance L(x) emitted from scene points is attenuated due to scattering caused by haze particles along the line of sight, and (ii) ambient airlight A is also scattered by haze particles, causing some of it to be reflected into the line of sight and reach the camera. The resulting image H(x) exhibits reduced contrast and distorted colors, and is typically modeled [4, 5, 6] by:

$$H(x) = T(x)F(x) + (1 - T(x))AL \quad [1]$$

where T(x) is the corresponding attenuation factor, known as the transmission

$$T(x) = e^{-\beta Y(x)} \quad [2]$$

where β is a scattering coefficient and Y(x) is the distance to the scene point. T(x) is typically assumed to be the same for all three color channels (R,G,B) [3, 4].

The main difficulty in solving single image dehazing is the double unknowns of the haze-free image F(x,y) and the scene depth D(x,y). Some previous work used multiple images of the same scene taken under different angles of polarization [7] or under different weather conditions [8] to derive a haze-free image. However, acquisition of multiple images may not be possible in real applications. On the other hand, some approaches did try to tackle the single image dehazing problem using either user-input vanishing point [9] or an accurate depth map [10]. The dehazing performance then highly depends on the accuracy of the given depth map.

Early methods utilize various priors to settle the ill-posed problem so that the image can be restored. He et al. [11] proposed the theory of dark channel prior (DCP) for the prediction of transmission map. Zhu et al. [12] reconstructs transmission map based on the observation of color attenuation prior (CAP). Those prior-based methods are not robust enough in real-world scene. Recently, learning based methods are more popular because of the rise of deep learning. Some of them use convolutional neural network (CNN) to estimate the parameter of the physical model and restore clear images. A common practice is to use deep neural networks to predict transmission maps from the hazy images [13] [14],

Sri Venkateswara College Of Engineering & Technology

there are also some networks designed to jointly predict the transmittance and the airlight [15] [16]. Since these methods are still limited to the dehazing model, when the parameters of the model are not accurately predicted, the removal performance is reduced. And for nonuniform weather conditions, they often fail to estimate the haze accurately, which in turn affects the subsequent dehazing.

This MOF is then embedded into patch-wise dehazing to suppress halo artifacts. Still, we perform post-processing methods to improve robustness and reduce computational complexity of the MOF using IRCNN.

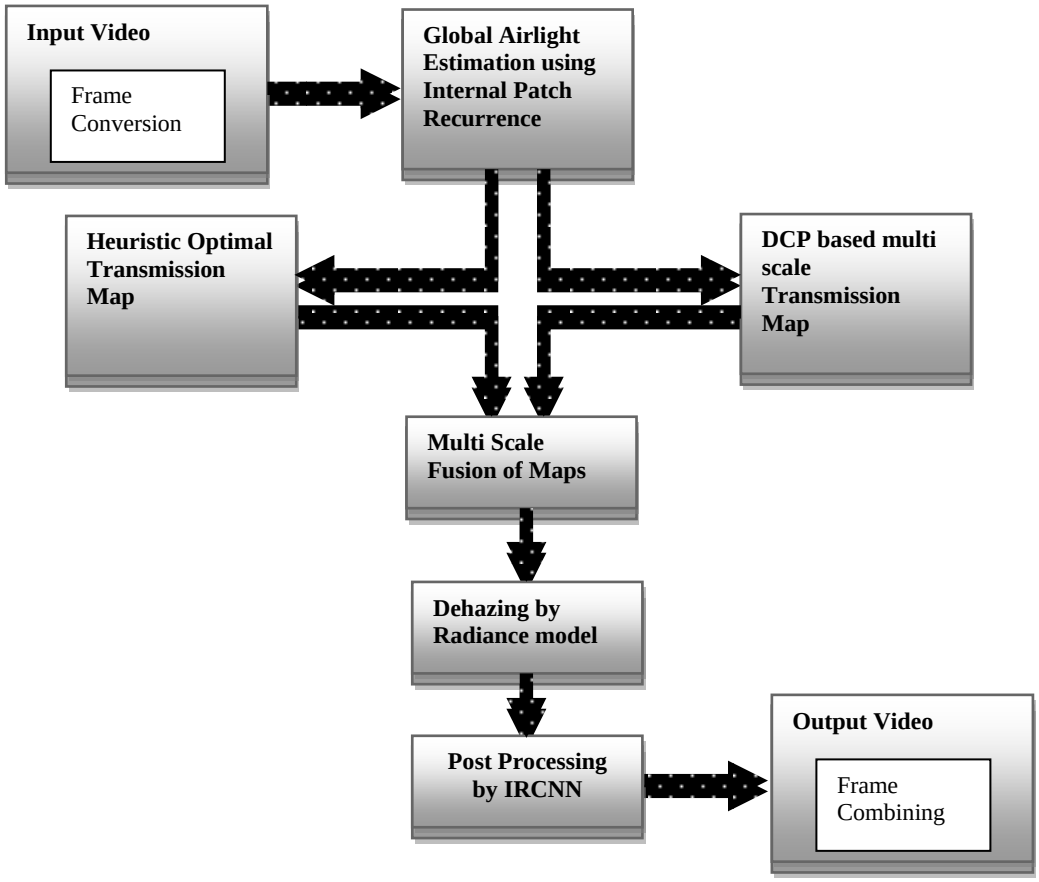

Figure 1. Block Diagram of Proposed System

To tackle this issue, different prior information has to be considered into the optimization framework such as dark channel prior [17], contrast color-lines [18]] and hazeline prior [19]. For example, based on the observation that there always exists one channel that is significant dark in the captured outdoor images, dark-channel prior [17] is leveraged in the optimization framework to guarantee dehazed images are "dark channel". Motivated by this observation, we propose to use the internal patch recurrence property as a strong prior for single-image blind dehazing. Small image patches (e.g., 5x5, 7x7) tend to repeat abundantly inside a single natural image, both within the same scale, as well as across different scales of the image. Then we derive an optimal transmission map under a locally constant assumption. To improve the estimation for white/black areas in a scene, we further include a transmission heuristic and formulate the image dehazing as solving the optimal transmission map under the transmission heuristic constraint. Finally Multi-scale Optimal Fusion (MOF) model is computed to fuse pixel-wise and patch-wise transmission maps optimally to avoid misestimated transmission region.

The rest of the paper is organized as follows. Section 2 gives the overall methodology of our proposed algorithm along with block diagram of implementation. In Section 3, the details of the proposed Airlight estimation using internal patch recurrence are presented. In section 4, Optimal transmission map estimation steps are explained. In Section 5, MOF model are presented, including TME region recognition, multi-scale transmission map estimation. A post-processing is presented along with MOF. In Section 6, the experimental metrics shows that the superior performance of the proposed. Section 7 holds the conclusion of entire system.

II. SYSTEM DESCRIPTION

The following is the methodology to remove haze from video.
1) Input the video
2) Extract the sequence of frames from the video
3) Process each frame as follows

4) Estimate the atmospheric light
5) Estimate the optimal transmission map
6) Compute the Refine Transmission map of multi scale
7) Perform the MOF for these two maps
8) Recover the scene radiance
9) Go to step 4 until the entire sequence of frames are processed
10) Combine dehazed frames into video
11) Output the video.

The complete block diagram of implementation is illustrated in Fig. 1. For every video to be process, we divide the videos into number of frames. Frames are nothing but the data structure of images which is captured on corresponding frame duration. So, this data structure is again converted to image format of matrix dimension with their resolution. After this, airlight estimation using internal patch recurrence is performed for any one of the extracted frame image. To reduce the time computation in the system we are performing the airlight estimation only for one frame that may be any of the video. Once this atmospheric light is computed, we are estimated the optimal transmission map using transmission heuristic procedure. For the same frame we calculated the number of transmission maps with different number of scales using DCP. These both the results are applied into MOF and obtained the combined and refined transmission map. Radiance image from refined transmission map is estimated to get the dehazed frame output. Finally we can combine all frames and get dehazed video output.

III. BLIND AIRLIGHT ESTIMATION

Nevertheless, degradation is not limited to blur; other types of degradations in the imaging process may also lead to diminished patch recurrence. Deviations from the ideal patch recurrence encode valuable information about the unknown degradation process, in general. In particular, images taken under bad weather conditions (haze, fog, etc.) suffer from diminished patch recurrence. Recurring patches at different depths undergo different amounts of haze, hence no longer look the same (e.g., see the patches P1 and P2 in Fig. 2). Nevertheless, these differences between such "co-occurring patches" (patches with high normalized correlation) allow recovery of their shared airlight color AL and their relative transmission parameters. Combining the information from a sparse set of co-occurring pairs of patches in the image, yields the global airlight color AL [20].

Figure 2. Co-Occuring Patches of image

The algorithm of airlight estimation used in our proposed system is explained as below.

Algorithm 1: Airlight estimation using internal patch recurrence

Input : Haze Frame H(x)
Output: Airlight AL

Step 1: Co-Occuring pairs prediction
- i. High variance patches extraction from image H(x)
- ii. Matching patches searching with high normalized correlation using equ [4].

Step 2: Pairwise haze parameter for each pair
- i. Relative t-values of pair T2/T1 using equ [5]
- ii. Shared airlight AL_k between P1 and P2 by equ [6]

Step 3: Global airlight estimate from all pariwise AL_k using equ [7]

Let P1[x] and P2[x] denote a pair of small co-occurring patches (7x7) that originate from the same underlying haze-free patch L[x]. According to equ [1],

$$P_1[x] = L(x)T_1 + AL_1(1 - T_1)$$
$$P_2[x] = L(x)T_2 + AL_2(1 - T_2) \quad [3]$$

For haze-free image, the patches P1 and P2 should be identical. However, due to the haze and their different depths, they look quite different as in Fig. 2. The concealing effect of the airlight AL is removed in the mean-free patches $\widehat{P1}$ and $\widehat{P2}$. However, their different transmissions still obscure their similarity. Therefore, we normalize the standard deviation of each patch, in the case of l2 norm.

$$\frac{\tilde{P}_1[x]}{\| \tilde{P}_1 \|} = \frac{T_1\tilde{L}[x]}{T_1 \| \tilde{L} \|} = \frac{\tilde{H}[x]}{\| \tilde{H} \|}$$
$$\frac{\tilde{P}_2[x]}{\| \tilde{P}_2 \|} = \frac{T_2\tilde{H}[x]}{T_2\tilde{H} \|} = \frac{\tilde{H}[x]}{\| \tilde{H} \|} \quad [4]$$

$$\frac{\tilde{P}_1}{\| \tilde{P}_1 \|} = \frac{\tilde{P}_2}{\| \tilde{P}_2 \|} \quad [5]$$

Thus, normalizing the mean-free version of all hazy image patches unveils their recurrence property. Pairs of co-occurring patches can now be detected by applying Nearest-Neighbors (NN) search on the normalized patches. Since our final goal is to recover a haze-free image with maximal patch recurrence across multiple scales, we search for normalized-NNs (co-occurring patches) across multiple scales of the input hazy image. Note that scaling down the hazy image does not change the physical parameters of the scene (the airlight at

infinity, the depth of scene points, or the haze scattering parameters); it only has a zoom-out effect. We apply NN-search only to patches which have high std (above 25 grayscale levels). Relative transmission parameter T1/T2 is the ratio between the transmission parameters of two co-occurring patches, P1 and P2. Recall that T1 and T2 are scalars (between 0 and 1). Thus it reduces to a simple ratio of their standard-deviations.

$$\frac{T_2}{T_1} = \frac{std(P_2)}{std(P_1)} \qquad [6]$$

The shared airlight can be estimated using least squares as,

$$AL = \frac{\left(\tilde{P}_2 - \tilde{P}_1\right)^T [P_1 \circ P_2 - P_2 \circ \tilde{P}_1]}{\| \left(\tilde{P}_2 - \tilde{P}_1\right) \|^2} \qquad [7]$$

where o denotes the element-wise vector multiplication (also known as the Hadamard product). Note that our recovery of the airlight AL does not require having scene points at infinity in the image.

The single global airlight estimate $\widehat{AL}$ for the entire image could in principle be computed as the average. Patch pairs of different depths are having high information than the similar depth patches. So, global airlight is estimated using weighted average as below,

$$\widehat{AL} = \frac{\sum_k \varphi_k \widehat{AL}_k}{\sum_k \varphi_k} \qquad [8]$$

giving higher weights φ_k to more informative pairs of patches. Informative pairs should have a very large pairwise t-ratio ($\frac{T1}{T2} \gg 1$). The weight of each pair can be derived as below

$$\varphi_k = \left[\left(T_{FB_1} - T_{FB_2}\right)\left(\frac{T_{FB_1}}{T_{FB_2}} - 1\right)\right]^2 \qquad [9]$$

This accomplishes the weighting effect, where T_{FB} is defined as,

$$T(x) \geq \max_{c \in R,G,B} \left\{1 - \frac{H_c(x)}{AL_c}\right\} \triangleq T_{FB}(x) \qquad [10]$$

We perform the iteration until the rate of change in $\widehat{AL}$ is very small which shows that this iterative weighting minimizes the estimation error by 25%.

IV. Optimal Transmission Map

To improve the estimation for white/black areas in a scene, we further include a transmission heuristic and formulate the image dehazing as solving the optimal transmission map under the transmission heuristic constraint [21]. The algorithm of transmission map estimation is as follows.

Algorithm 2: Optimal Transmission Map using Heuristics

Input : Haze Frame H(i), Airlight AL

Output: Optimal Transmission Map T

1. Obtain T from AL of algorithm 1.
2. Calculation of γ from equ [12]
3. Optimal γ computing using equ [14]
4. Objective function heuristic for using equ [18]
5. Quadratic programming for optimal T map using equ [19]

Our goal is to approximate the two unknowns: the transmission T(x) and the haze-free image L(x). Rewriting equ [1] as,

$$T(x,y) = \frac{1}{F(x,y) - AL} H(x,y) + \frac{-AL}{F(x,y) - AL} = \gamma(x,y)[H(x,y) - AL] \qquad [11]$$

Where,

$$\gamma(x,y) = \frac{1}{F(x,y) - AL} \qquad [12]$$

Thus, for each pixel i in a local window w, we have a constant γ:

$$T_i \approx \gamma^c [H_i^c - AL^c], \forall_c \in (r,g,b) \qquad [13]$$

Where, c denotes the color channel. Under the locally constant assumption, our goal becomes to find T and γ by minimizing the following cost function,

$$C(T,\gamma) = \sum_k \| Y_k \gamma_k - M\bar{T}_k \|^2 \qquad [14]$$

Where,

$$\gamma_k = \left[\gamma_k^r, \gamma_k^g, \gamma_k^b\right]^T \qquad [15]$$

Y_k is defined as 3x3 matrix as,

$$Y_k = \begin{bmatrix} T^r & & \\ & T^g & \\ & & T^b \\ \varepsilon & & \\ & \varepsilon & \\ & & \varepsilon \end{bmatrix} \qquad [16]$$

where Tc is a $|w_k| \times 1$ vector containing in each entry for all i ϵ w_k, ε is a regularization parameter for γ and M is a $3(|w_k|+1) \times (|w_k|+1)$ matrix defined by:

$$M = \begin{bmatrix} H_{|w_k|\times|w_k|} & 0 \\ H_{|w_k|\times|w_k|} & \vdots \\ H_{|w_k|\times|w_k|} & \vdots \\ 0 & 0 \end{bmatrix} \quad [17]$$

Similarly, after first deriving the optimal γ_c , we obtain the final objective function:

$$C(T) = \sum_k \bar{T}_k^T \overline{AL}_k^T \overline{AL}_K \bar{T}_K = T^T \cup T \quad [18]$$

Where,

$$\overline{AL}_k = M - Y_k\left((Y_k^T Y_k)\right)^{-1} Y_k^T M \quad [19]$$

The transmission value of this object should be larger than the transmission heuristic because the object is closer to the camera than the background. Given an image, we first detect the horizontal line and then determine the transmission heuristic for the ground area according to its vertical distance from the horizon. The transmission heuristic for the sky area (i.e. above the horizon) is all set to 0. Moreover, we add a smoothness term on T so that the transmission of a certain object should be nearly constant. By including the above constraints, we finally obtain a constrained quadratic equation, which can be optimized by quadratic programming and have a global optimum solution:

$$C(T) = T^T \cup T + \xi \parallel \nabla \mathrm{T} \parallel^2 \quad [20]$$
$$s.t. max\left(h_j, \frac{AL - E_j}{AL}\right) \le T_j \le 1, \forall j \in E$$

where, hj is the transmission heuristic of the jth pixel, and ξ is a factor to control the effect of smoothness term. The upper bound of α is set as 1 to satisfy the exponential function.

V. MULTI SCALE OPTIMAL FUSION OF TRANSMISSION MAP

Pixel-wise transmission map estimation method is free of halo artifacts. However, it always overestimates haze intensity beyond its actual value, which leads to over-saturated haze removal image although the patch-wise dehazing could refrain from over-saturation, it may result in halo artifacts. Multi-scale Optimal Fusion (MOF) model to fuse pixel-wise and patch-wise transmission maps optimally to avoid misestimated transmission region. This MOF is then embedded into patch-wise dehazing to suppress halo artifacts [22].

As discussed above, patch-wise dehazing would result in halo artifacts around the edge with abrupt grayscale change, namely TME region. So pixel-wise instead of patch-wise dehazing is expected in TME region. For this purpose, the ideal transmission map T_{mof} is computed by,

$$T_{mof}(x) = \chi_{tme}(x).T_{pi}(x) + \chi_{\overline{tme}}(x).T_{pa}(x) \quad [21]$$

where T_{pi} and T_{pa} represent transmission maps of pixel-wise and patch wise, χ_{tme} and $\chi_{\overline{tme}}$ give the weights for combining T_{pi} and T_{pa}.

To get an ideal transmission map, we should minimize the difference between $T_{mof}(x)$ and $T_{pi}(\boldsymbol{x})$ inside the TME region, and minimize the difference between $T_{mof}(x)$ and $T_{pa}(x)$ outside the TME region, i.e.

$$\chi_{\overline{tme}}(x) \approx 0 \; and \; \chi_{tme}(x) \approx 1, x \in TME$$
$$\chi_{\overline{tme}}(x) \approx 1 \; and \; \chi_{tme}(x) \approx 0, x \notin TME \quad [22]$$

TME region can be roughly extracted by following method:

$$B_t = max\left[\left(1 - \Omega D_{pa}\right) - \left(1 - \Omega D_{pi}\right), 0\right] \quad [23]$$

Where, Ω is application-based constant used to adaptively keep more haze for the distant objects [23], D_{pi} and D_{pa} are the dark channels calculated by pixel-wise and patch-wise estimations, respectively.

Patch wise transmission map is computed from DCP and pixel wise transmission map is computed using optimal transmission map of algorithm 2. Texture smoothing and contrast enhancement of each patch is carried out using Gaussian filtering and tanh functions respectively. we finally obtain the χ_{tme} = B_f and $\chi_{\overline{tme}}$= 1 − B_f , respectively.

To do this, we first estimate the Tpaj for different patch size pj (j = 1, 2,...β). The choice of pj depends on image resolution that

$$p^j = \lfloor 2j \,.\log(w \times h) \rfloor - 1, \qquad j = 1,2,3 \ldots . \beta \quad [24]$$

where $\lfloor \cdot \rfloor$ is a rounded down function, and w and h are the width and height of the input image, respectively. β is the number of scales. Then, according to ideal transmission map fusion [22] ,

$$T_{mof}(x) = \frac{B_f(x).T_{pi}(x) + \left(1 - B_f(x)\right).T_{pa}(x) + \lambda_t}{B_f^2(x) + \left(1 - B_f(x)\right)^2 + \lambda_t} \quad [25]$$

Different scales of transmission map (T_{mof}^j) are calculated from equ [25]. Finally, all these transmission maps are fused together to give a multi-scale transmission map through

$$T_{mof} = \sum_j^{\beta} v^j T_{mof}^j, \; j = 1,2,3 \ldots . \beta \quad [26]$$

where T_{mof} is the fused transmission map, $\boldsymbol{v}j$ is the weight for the jth scale, conforming to $\Sigma\beta j \; \boldsymbol{v}j$ = 1, which is defined by,

$$v^j = \frac{e^{\rho}|p(\beta - j + 1) - 1|}{\sum_i^{\beta} e^{\rho \,.|q(i) - 1|}}, j = 1,2,3 \ldots . \beta \quad [27]$$

where qj is the patch size of the jth scale, ρ is the proportional control factor. The larger ρ indicates more uneven of the weights. For suppressing textures in a transmission map, a fast

GD-GIF is further imposed on the output of MOF refined T-map.

The flow of MOF model is illustrated in below fig. 3.

To evaluate the proposed MOBliF method, we are considered the multiple test videos in the condition of low haze, medium haze and high haze. Natural haze videos are tested and even synthetic haze video is evaluated. To illustrate the adaptive performance of our system we checked for underwater video

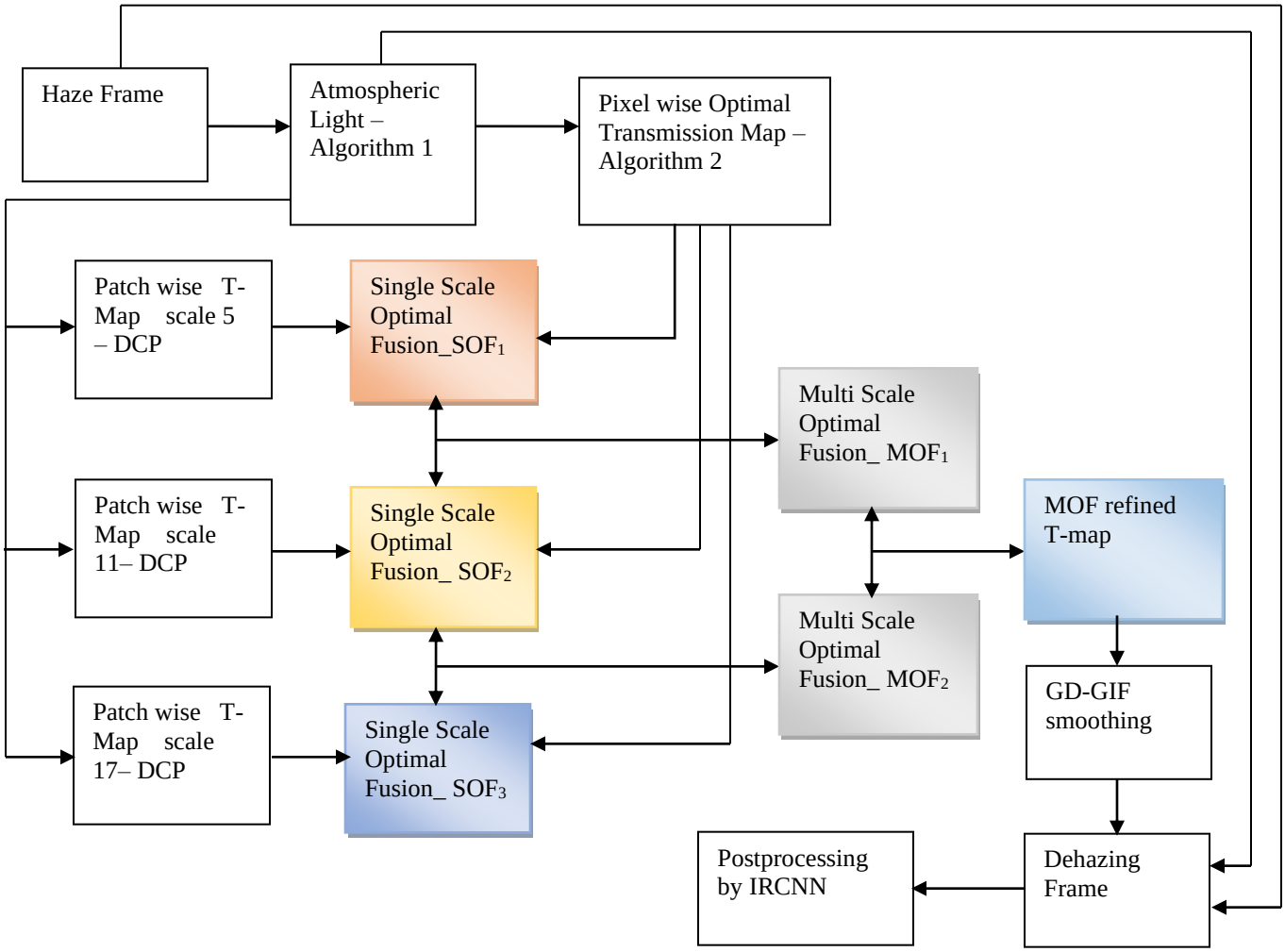

Figure 3.Entire Work flow of our proposed MOBliF

A. *Post Processing*

The image after haze removal looks so dark that image details cannot be seen clearly. This is because transmission map of the MOF is always less than patch-wise. To address this problem, the dehazed image is further adjusted by an adaptive exposure scaling [24]. For effective dehazing process, we included the IRCNN based denoising for enhanced frame result[25].

VI. PERFORMANCE ANALYSIS

also in this evaluation. Videos which we considered are having different resolution and frame duration. Recent three existing methods are taken for comparison with our method named as Non-local Video Dehazing [26], Multi Scale CNN [27], MLP dehazing [28]. We are estimated the qualitative and quantitative metrics for performance analysis.

Figure 4. Haze Frame

Fig 4 shows the input frame which we considered for the processing of dehazing. For sample we depicts the results of only frame for all steps of implementation MOBliF algorithm.

In fig. 5., (a),(b),(c), we shown the transmission maps computed in our algorithm. The Transmission map optimization places the major role in the dehazing process. In our method we used two different transmission map estimation.

One from the optimal transmission heuristic based Map estimation to detect the adaptive transmission content in frame which is illustrated in Fig5.(a).

(a) Optimal Transmission Map

(b) DCP transmission Map of Scale 5

(c) DCP transmission Map of Scale 11

Figure 5. Transmission Maps of Optimal and Multi Scale DCP

Another Transmission Maps are called as Multi scale transmission maps. To produce these maps we taken the scales for patch size. In our evaluation we are taken patch size as 5,11,17. As patch size getting increase the zooming effect of transmission map computation will increase. For example we depicts the two different scales of 5 and 11 based transmission map which derived from DCP algorithm in fig. 5-b) and 5-c) respectively. From these figures we can noticed that fig.5-b) transmission map is somewhat better resolution than 5-c). According to these qualitative results we can conclude that with small patch size, we will get high resolution transmission maps.

a) Optimal Map

b) MOF refined Map

Figure 6. Refinement of Transmission Map by optimal MOF

Fig. 6. Shows how the optimal map and multi scale transmission maps are fused to produce the effective transmission map for attain quality of dehazed image.

(a) **(b)**

Figure 7.(a) Haze Frame (b) Dehaze Frame of our proposed MOBliF

Figure 4, illustrates the qualitative result of dehazing frame output from our proposed algorithm.

For quantitative analysis of the proposed algorithm and existing methods we are considered performance metrics which are calculated between haze free frame and dehazed frame. The parameters we are taken for the experiment evaluations are as below

- PSNR
- MSE
- SSIM
- Computation time
- Haze Level
- Haze Intensity
- Contrast-to-Noise Ratio
- Gain of Visibility level
- SSEQ
- UQI
- BAQI
- CEIQ

Table 1, shows the measures which are derived from proposed dehazed output and existing outputs. Each metric decides the efficiency of the system for video dehazing

Table 1. Quantitative Performance metrics evaluation for proposed and existing methods

Methods	PSNR (dB)			(sec)	Level(%)	Intensity		Visibility			BAQI	CEIQ
Non-Local[26]	17.96	1042.13	0.75	**0.25**	35.35	90.14	1	11.37	26.54	142.73	0.01	3.32
MSCNN [27]	19.51	730.95	0.89	0.34	62.20	158.60	1	8.11	16.95	152.20	0.01	3.16
MLP [28]	17	1335.58	0.83	0.45	33.91	86.47	1.05	17.61	16.59	158.19	0.01	3.01
Proposed MOBliF	**22.2**	**0.03**	**0.95**	0.46	**66.43**	**169.39**	**1.89**	**87.87**	**28.62**	**159.43**	**0.11**	**3.44**

VII. CONCLUSION

This paper proposed the new efficient video dehazing framework using optimized multi scale fusion along with effective airlight estimation. The traditional dehazing method was enhanced in order to make the dehazing process fast while maintaining a dehazing quality. For this purpose, the airlight estimation is performed based on blind internal patch recurrence and transmission maps are fused by Multi Scale Fusion of pixel wise transmission map and patch wise transmission maps. Pixel wise transmission map is obtained from optimal heuristic transmission map which overcome the oversaturation and halo artifact effects in the dehazing of the video frame. In order to further improve the quality of the output we used IRCNN to restore the frame from any of the distortion and noises. Experiments were conducted on multiple datasets (synthetic and real) and the results were compared against several recent methods. Significance of the proposed system implementation is measure and proven that our results achieved the best performance. For future applications, we can try to reduce the time complexity by using digital signal processing hardware unit integration to compactly connect with real time scenarios.

REFERENCES

[1] Rahul Kumar, Raman Balasubramanian and Brajesh Kumar Kaushik , “Efficient Method and Architecture for Real-Time Video Defogging”, IEEE TRANSACTIONS ON INTELLIGENT TRANSPORTATION SYSTEMS, 2020

[2] Yuval Bahat, Michal Irani,” Blind Dehazing Using Internal Patch Recurrence”, Israel Science Foundation, 2014

[3] R. Fattal. Single image dehazing. In ACM Transactions on Graphics (TOG), volume 27, page 72, 2008.

[4] K. He, J. Sun, and X. Tang. Single image haze removal using dark channel prior. PAMI, 33(12):2341–2353, 2011.

[5] Y. Y. Schechner, S. G. Narasimhan, and S. K. Nayar. Instant dehazing of images using polarization. In CVPR, 2001.

[6] M. Sulami, I. Glatzer, R. Fattal, and M. Werman. Automatic recovery of the atmospheric light in hazy images. In ICCP,pages 1–11, 2014.

[7] S. Shwartz, E. Namer, and Y.Y. Schechner. Blind Haze Separation. Proc. IEEE Conf. Computer Vision and Pattern Recognition, vol. 2, pp. 1984–1991, 2006.

[8] S.G. Narasimhan and S.K. Nayar. Contrast Restoration of Weather Degraded Images. IEEE Trans. Pattern Analysis and Machine Intelligence, vol. 25, no. 6 pp.713–724, June 2003.

[9] S.G. Narasimhan and S.K. Nayar. InteractiveDeweathering of an Image Using Physical Models. Proc. IEEE Workshop on Color and Photometric Methods in Computer Vision, pp. 1387–1394, Oct. 2003.

[10] J. Kopf, B. Neubert, B. Chen, M. Cohen, D. Cohen-Or, O. Deussen, M. Uyttendaele, and D. Lischinski. Deep photo: Model-Based Photograph Enhancement and Viewing. ACM Trans. Graphics, vol. 27, no. 5, pp.116:1–116:10, 2008.

[11] Kaiming He, Jian Sun, and Xiaoou Tang. Single image haze removal using dark channel prior. IEEE transactions on pattern analysis and machine intelligence, 33(12):2341–2353, 2011.

[12] Qingsong Zhu, Jiaming Mai, and Ling Shao. A fast single image haze removal algorithm using color attenuation prior. IEEE transactions on image processing, 24(11):3522–3533, 2015.

[13] Wenqi Ren, Si Liu, Hua Zhang, Jinshan Pan, Xiaochun Cao, and Ming-Hsuan Yang. Single image dehazing via multiscale convolutional neural networks. In European conference on computer vision, pages 154–169. Springer, 2016.

[14] Bolun Cai, Xiangmin Xu, Kui Jia, Chunmei Qing, and Dacheng Tao. Dehazenet: An end-to-end system for single image haze removal. IEEE Transactions on Image Processing, 25(11):5187–5198, 2016.

[15] Hongyuan Zhu, Xi Peng, Vijay Chandrasekhar, Liyuan Li, and Joo-Hwee Lim. Dehazegan: When image dehazing meets differential programming. In IJCAI, pages 1234–1240, 2018.

[16] Xitong Yang, Zheng Xu, and Jiebo Luo. Towards perceptual image dehazing by physics-based disentanglement and adversarial training. In Thirty-second AAAI conference on artificial intelligence, 2018.

[17] K. He, J. Sun, and X. Tang, "Single image haze removal using dark channel prior," IEEE Trans. on PAMI, vol. 33, no. 12, pp. 2341–2353, 2011.

[18] Dehazing using color-lines," vol. 34, no. 13. New York, NY, USA: ACM, 2014.

[19] D. Berman, S. Avidan et al., "Non-local image dehazing," in CVPR, 2016, pp. 1674–1682.

[20] Q. Zhu, J. Mai, and L. Shao. A fast single image haze removal algorithm using color attenuation prior. IEEE Transactions on Image Processing, 24(11):3522–3533, 2015

[21] Yi-Shuan Lai, Yi-Lei Chen, and Chiou-Ting Hsu," Single Image Dehazing With Optimal Transmission Map", 21st International Conference on Pattern Recognition (ICPR 2012) November 11-15, 2012. Tsukuba, Japan

[22] Dong Zhao, Long Xu, Yihua Yan, Jie Chen, Ling-Yu Duan," Multi-scale Optimal Fusion model for single image dehazing", Signal Processing: Image Communication 74 (2019) 253–265

[23] K. He, J. Sun, X. Tang, Single image haze removal using dark channel prior, IEEE Trans. Pattern Anal. Mach. Intell. 33 (12) (2011) 2341.

[24] K. Tang, J. Yang, J. Wang, Investigating haze-relevant features in a learning framework for image dehazing, in: IEEE Conference on Computer Vision and Pattern Recognition, 2014, pp. 2995–3002.

[25] Zhang, Kai and Zuo, Wangmeng and Gu, Shuhang and Zhang, Lei, "Learning Deep CNN Denoiser Prior for Image Restoration",IEEE Conference on Computer Vision and Pattern Recognition,3929-3938,2017

[26] Dana Berman, Tali Treibitz, Shai Avidan, "Non-Local Image Dehazing", IEEE 2015.

[27] Wenqi Ren, Si Liu, Hua Zhang,Jinshan Pan, Xiaochun Cao and Ming-Hsuan Yang, "Single Image Dehazing via Multi-scale Convolutional Neural Networks", Springer International Publishing: ECCV 2016, Part II, LNCS 9906, pp. 154–169, 2016.

[28] Sebastián Salazar, Ivan Cruz-Aceves, Juan-Manuel Ramos-Arreguin," Single image dehazing using a multilayer perceptron", J. of Electronic Imaging, 7(24), 2018). https://doi.org/10.1117/1.JEI.27.4.043022